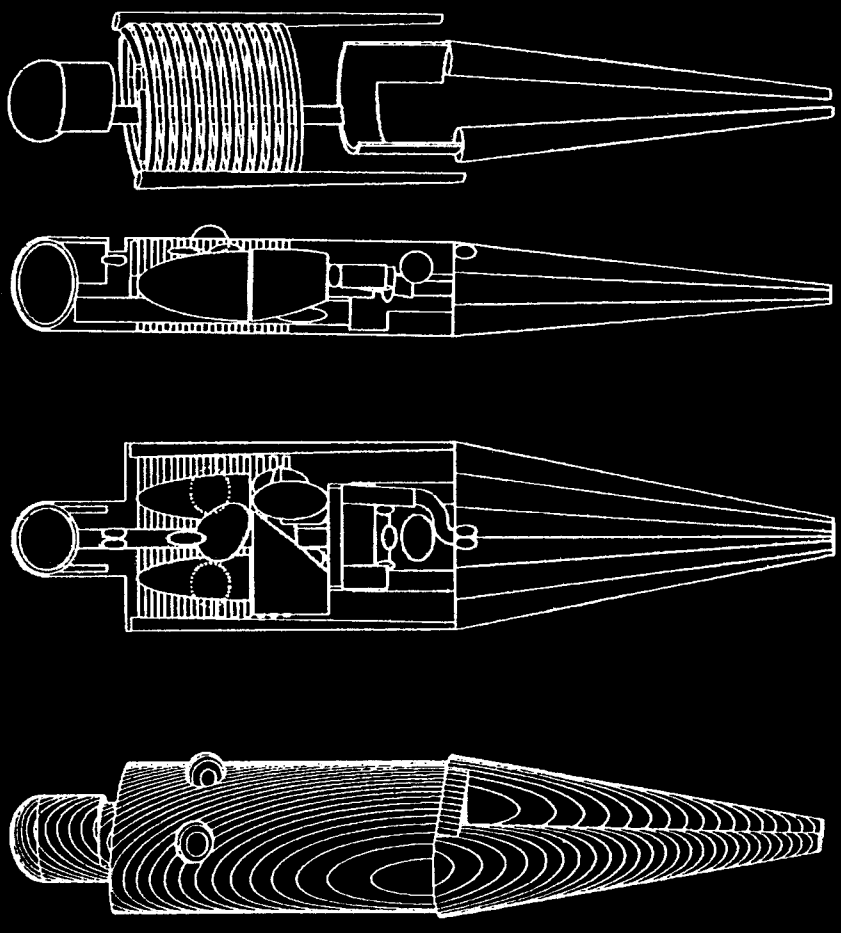

Practical Radiation Protection

In Health Care

Edited by
C. J. Martin and D. G. Sutton

14.6 Dose calculation

14.6.1 Calculating dose from technique factors

It is a simple matter to calculate the entrance air kerma without backscatter (incident air kerma) at the point where the central ray enters the patient. The information required is the kV, mAs, and focus–patient distance.

$$\text{IAK} = [\text{output} \times \text{mAs}]/\text{FSD}^2 \text{ mGy}$$

where IAK is the incident air kerma, output is the air kerma per mAs at 1 m (in mGy mAs^{-1}) at the kV used, mAs is the product of X-ray tube current and exposure time, and FSD is the distance from the focus to the surface of the patient, in metres.

Output can be measured using an ionisation chamber or other instrument with suitable properties. Errors can occur if the output is not measured under exactly the same conditions as the clinical exposures. For example, significant differences may exist between broad and fine focus and between different mA stations. In addition, in the case of retrospective calculations the FSD is unlikely to be known, and the individual kV and mAs may also not have been recorded. (Whether or not the resultant error is significant will depend on the purpose of the dose estimations and will require some professional judgement.) For retrospective calculations, in the absence of direct measurements, quality control output data may be usable. Where output data at the kV used (kV_{Pat}) are not available, an adjustment can be made based on the proportionality to the square of the kV.

$$\text{IAK} = [\text{output}_{kV_0} \times \text{mAs} \times (kV_{Pat}/kV_0)^2]/\text{FSD}^2 \text{ mGy}.$$

As a last resort published output data can be utilized.

Clearly, the difference between a direct measurement of ESD, using TLD for example, and this method is the inclusion of backscatter in the former. Care needs to be taken when comparing data from different sources in establishing whether backscatter has been included, and in what medium dose has been calculated (e.g. water, air, ICRU muscle, etc.). The backscatter factor depends on beam quality and examination conditions, such as beam size and part of body being irradiated. For thick body parts the backscatter factor will be in the region of 1.35 ± 10% (Table 14.1).

14.6.2 Monte Carlo methods for estimating organ and effective doses

Monte Carlo techniques have been used extensively in diagnostic radiology to investigate patient doses and image quality. In summary, the method involves the computer simulation of the transport of X-ray photons through the patient, selecting photons at random from the relevant spectral distribution, and using cross-section data for the various interaction processes. Several million photons may need to be tracked in order to give acceptable statistical accuracy in the calculated quantities, such as absorbed dose in a particular organ. The patient is represented by a mathematical phantom, in which the various body parts, tissues, and organs are modelled by simple mathematical shapes of appropriate composition (Figure 14.2). Phantoms derived from cross-sectional data provided by CT or magnetic resonance (MR) images have also been developed [12]. Space does not permit a detailed discussion of the method: the interested reader is recommended to consult reviews or other texts [16, 17]. Monte Carlo techniques are generally used where analytical methods are unavailable or impractical. They have the advantage that results can be generated relatively easily for a wide variety of scenarios. Such results may be almost impossible to obtain by direct measurement or at best would be exceedingly time-consuming to collect.

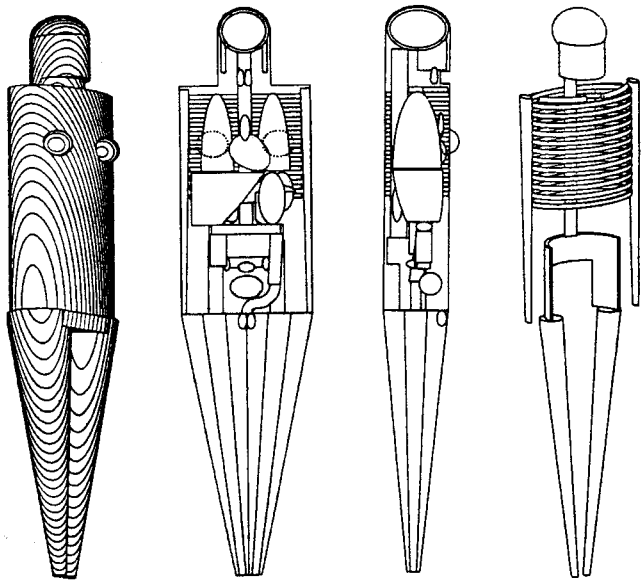

Figure 14.2 External, internal, and skeletal views of the hermaphrodite mathematical phantom used by Jones and Wall [18]. (Reproduced courtesy of NRPB.).

For the purposes of this chapter, the most useful form of the results generated by Monte Carlo programs is in terms of normalized organ doses, that is, organ dose per unit ESD or incident air kerma. There are a number of published compilations of normalized doses for common radiological procedures, which can be used in most circumstances.

The most extensive data, in terms of numbers of projections and organs included, are those which have been produced by the UK National Radiological Protection Board (NRPB). They used an adult hermaph-

rodite phantom, based on the MIRD-5 phantom [18]. Factors for estimating effective dose from ESD and DAP are given in NRPB-R262 [1] for 68 common X-ray projections and 40 X-ray spectra. Complementary software also gives normalized doses to all the ICRP and remainder organs [19]. In addition, the NRPB have produced similar information for children of ages 0, 1, 5, 10, and 15 years [2], and for adult CT examinations [20] (§14.8). The specifications for the mathematical phantoms mentioned above, along with a number of others, have been summarized in ICRU Report 48 [12]. A number of authors have published factors to convert entrance air kerma (or similar) to mean glandular dose for mammographic examinations and these are discussed in §14.9.1.

A problem which may be encountered when using published Monte Carlo data is the absence of data for the examination, projection, or field size under consideration. Nevertheless, it may still be possible to find an adequate match for most purposes, although it should be noted that there can be substantial differences for organ and effective doses between AP and PA projections, and between left and right laterals.

Errors will also be incurred due to differences between patient and phantom dimensions, and the positions and sizes of organs. Such errors are difficult to quantify, especially if a small organ is near to the edge of the primary beam, in which case small changes in beam or organ position can significantly affect the dose. The magnitude and sources of uncertainties in different circumstances have been discussed in [18].

14.7 Dosimetry in radiography and fluoroscopy

The following sections give some indications of how the techniques described above can be applied in common situations to estimate effective dose and relevant organ doses. The Monte Carlo methods for estimating organ doses take into account the different compositions of different organs. This is usually straightforward, except for bone, where calculation of bone marrow dose has to take into account the elevated dose due to photoelectrons generated in the surrounding high atomic number bone (Box 14.5).

14.7.1 Radiography

Patient dose estimations for radiographic exposures are usually relatively straightforward. For effective dose and organ doses the most convenient method would be to use the Monte Carlo generated data described in §14.6.2. Key requirements as input for the calculation are details of the examination and projection, the X-ray tube voltage (kVp), tube filtration, and the incident exposure, either in terms of ESD or DAP. Sometimes information on mAs may be unavailable if automatic exposure control (AEC) is used, although most new X-ray equipment now gives post-exposure readout of mAs. An alternative would be to use typical values employed in the department, taken from the exposure charts and possibly modified if the patient is known to be particularly large or small.

For simple radiographic examinations DRLs have been defined primarily in terms of ESD, with backscatter. However, much new X-ray equipment is provided with DAP meters, and by estimating the field size at the patient it is possible to convert from one quantity to the other. It is also possible to obtain DAP meters which use ultrasound to measure the distance to the patient, hence enabling entrance air kerma as well as DAP to be obtained. In the UK, publication of the *National protocol for patient dose measurements in diagnostic radiology* [22] was instrumental in initiating routine measurements of patient dose for comparison with DRLs. Typical patient doses and the current UK national DRLs for a range of examinations are given in Table 14.3.

When a patient receives a dose which may be 'much greater than intended' (Box 14.3), arising from an

Box 14.5 Bone dosimetry

The sensitive parts of trabecular bone, as far as cancer induction is concerned, are the bone surfaces and bone marrow. Because of the complex structure of trabecular bone, the calculation or measurement of dose to these tissues is extremely difficult. The dose to both the endosteal tissues and the marrow is enhanced as a result of photoelectrons produced by photoelectric interactions in the high atomic number bone. The dose enhancement depends on the distance of the sensitive tissues from the bone and is therefore higher for the endosteal tissues, which lie within 10 μm of the bone surfaces, whereas the marrow cavities vary from 50 μm to 2000 μm in size. Another factor to consider is the shielding effect of bone, which reduces the dose to tissues beyond (as well as to the soft tissues within the bone itself). In fact, for the dose to bone marrow, the shielding effect may outweigh the enhancement effect. Spiers [21] discusses bone and bone marrow dosimetry at much greater length, and gives tables of dose enhancement factors for different bones, at different ages, and for a range of X-ray energies. On average, the marrow dose enhancement is about 10% in the diagnostic energy range, whereas the enhancement to endosteal tissues is over 100%, except at the highest X-ray energies.

Table 14.3 Typical patient doses and provisional diagnostic reference levels for radiographic procedures

Examination		Entrance surface dose (mGy)	Dose–area product (Gy cm^2)	Effective dose (mSv)	Diagnostic reference level[a] (mGy)
Limbs and joints (except hip)				<0.01	
Chest	PA	0.16	0.08	0.02	0.2
	Lat	0.37	0.24	0.04	0.7
Skull	AP/PA	3.0	0.75	0.03	4
	Lat	1.5	0.37	0.01	2
Cervical spine				0.08	
Hip				0.3	
Thoracic spine	AP	4.7	1.7	0.4	5
	Lat	13.0	2.6	0.3	16
Pelvis	AP	4.4	4.0	0.7	5
Abdomen	AP	5.6	5.6	0.7	7
Lumbar spine	AP	6.1	2.6	0.7	7
	Lat	16.0	2.7	0.3	20
	LSJ	29.0	2.9	0.3	35
IVU (kidneys and bladder)			13.4	2.5	25[b]

[a]Entrance surface dose.
[b]Dose–area product (Gy cm^2).

equipment fault or human error, it is necessary to obtain an estimate of the patient dose. Initially, the requirement is to establish by what factor the actual dose exceeded the intended dose. It may be possible to make an adequate estimate by comparing mAs values, or DAP readings, for example. Assuming the exposure needs to be repeated to obtain a diagnostic film, the intended dose is best based on the factors used for the repeat film or from previous films taken on the same patient. A relatively common equipment fault is the failure of the AEC to correctly terminate the exposure. The operator may realize that something is wrong and release the handswitch, or the exposure may be terminated by the back-up timer. In either case the actual mAs given will probably be known. If it is not available a crude estimate of exposure time may be all that is possible. Alternatively, if the film is not completely black the increased dose may be estimated from the film density. If this initial investigation shows that the dose was 'much greater than intended', then a detailed estimate of effective dose is required, using the methods already described.

14.7.2 Fluoroscopy and fluorography

It is generally more difficult to estimate the dose to patients from image intensifier based examinations, mainly because the field size and projection tend to vary throughout the examination. In addition, exposure factors also vary and are less likely to be known: screening time and number of films, or digital images, may be the only parameters recorded. However, for prospective measurements, such as one-off dose surveys or special projects, it may be feasible to record complete information. The total examination can be divided into a number of discrete projections, and organ doses estimated for each projection, using the methods described in §14.7.1. Since most fluoroscopic equipment is fitted with DAP meters, doses will most conveniently be based on DAP meter readings for each projection. Strictly speaking, calculation of effective dose should then be based on the total doses to each organ over the complete examination, and should not be derived by summing the separate effective doses for each projection. This is because of the possibility of one of the remainder organs receiving the highest dose. If calculations are being performed using purpose-written software, such as that provided as an adjunct to the NRPB compilations [19], then this approach is straightforward. If, however, such software is not being used, it is often easier to sum the effective dose for each projection and make an estimate of the error involved. Care may be needed if the projections and field sizes used do not coincide with those available in the literature. However, several publications do give normalized organ doses appropriate to fluoroscopic procedures [1, 23, 24].

For retrospective dose estimations it may be necessary, and easiest, to determine the doses by simulating the examination using a phantom. If phantom measurements are undertaken care needs to be taken to reproduce clinical conditions as closely as possible, since exposure parameters are usually automatically controlled and can be quite critical on the techniques used.

DRLs for examinations involving fluoroscopy can be specified in terms of DAP, and UK national DRLs that have been set for barium enemas and barium meals are given in Table 14.4. Studies of more complex diagnostic and interventional procedures have taken place, and

Table 14.4 Typical patient doses and provisional diagnostic reference levels for fluoroscopy procedures

Examination	Dose–area product (Gy cm^2)	Effective dose (mSv)	Diagnostic reference level[a] (Gy cm^2)
Barium swallow	9.8	1.5	
Barium meal	13.0	3	17
Barium follow	12.0	3	
Barium enema	25.8	7	35

[a]Dose–area product.

should provide useful information in this developing area. At present, local dose surveys should be undertaken both for local guidance and to contribute to the setting of national levels. Since most dosimetry in fluoroscopic procedures is based on DAP readings, it is important that DAP meters fitted to equipment are calibrated regularly (Box 14.4). Some manufacturers display DAP readings based on calculation rather than direct measurement, and calibration is particularly important in these cases to allow for changes in X-ray output. Corrections may also need to be made for any special or additional tube filtration such as copper which may be introduced into the beam during an examination with the aim of reducing patient ESD.

With some lengthy interventional procedures it is possible to deliver skin doses high enough to cause deterministic effects, ranging from mild transient erythema to secondary ulceration (§11.3.3). Skin doses of up to 20 Gy have been reported. Normally, patient skin dose rates will be in the range 20–50 mGy min^{-1}, but could exceed 100 mGy min^{-1} under certain conditions: in fact UK legislation requires the dose rate at the surface of the skin not to exceed 100 mGy min^{-1}. Measurements should be undertaken to see if there is likely to be a problem, and where areas of the skin could receive more than about 1 Gy, such areas, along with dosimetric information, should be recorded for individual patients. Skin dose measurements on patients suffer from the difficulties already mentioned for fluoroscopy, particularly not knowing beforehand which area of skin will receive the highest dose. The options include placing one or more TLDs at appropriate positions on the patients or using one of the commercial instruments designed for this purpose (§14.5). Measurements of incident radiation derived from DAP readings could be used. They do not take into account the variation of beam position on the skin but would at least indicate the maximum possible skin dose.

14.8 Computed tomography

It is well recognized that CT delivers some of the highest doses to patients, compared with other radiological techniques. In the UK, although CT accounted for only about 4% of all procedures, its contribution to the collective effective dose due to diagnostic radiology was approximately 40% in 1998 and may now be greater. Estimation and control of doses in CT is therefore particularly important.

14.8.1 Computed tomography dose index (CTDI)

Because of differences between conventional radiography and CT, in particular in the shape of the X-ray beam and geometry of irradiation, it is not possible to use the same practical methods for assessing patient dose. ESD, with backscatter, can be measured with TLDs placed at appropriate locations on the patient's skin surface or on a suitable phantom. Various quantities, such as multiple scan average dose (MSAD) and multi-slice surface dose (MSSD), have been introduced to describe the average surface dose, over a slice width, from a series of contiguous slices. However, it is not easy to convert such a measurement to organ doses or effective dose, and it is not currently being proposed as a suitable quantity for DRLs in CT. Instead, it is usual to base CT dosimetry on measurements of the CTDI, a quantity which is a measure of the total dose from a single slice, and which is effectively a combination of tube output and slice width collimation. It is defined in general terms as:

$$\mathrm{CTDI} = 1/nT\int_{z_1}^{z_2} D(z)\,\mathrm{d}z$$

where z_1 and z_2 are the limits of integration, $D(z)$ is the single-slice dose profile, T is the nominal slice thickness in cm, and n is the number of slices irradiated simultaneously (for multi-slice CT).

CTDI is usually measured with a pencil ionisation chamber. The chamber is positioned parallel to the scanner axis at the centre of the field and a measurement taken for a single slice. The measurement performs the necessary integration, with limits determined by the length of the chamber. The length commonly used is 100 mm, and a number of suitable chambers are available commercially.

In terms of the chamber reading the CTDI is therefore given by

$$\mathrm{CTDI} = D \times F \times L/T \qquad \mathrm{mGy}$$

where D is the chamber reading in mGy, F is a factor to convert the chamber dose quantity to dose in the medium required, and L and T are the length of the ion chamber and the nominal slice thickness, respectively. F is unity in air and for other media is given by the ratio of the mass energy transfer coefficients in air and the appropriate medium: $(\mu_{en}/\rho)_{medium}/(\mu_{en}/\rho)_{air}$ (§2.7.4). The quantity is therefore energy dependent and it is

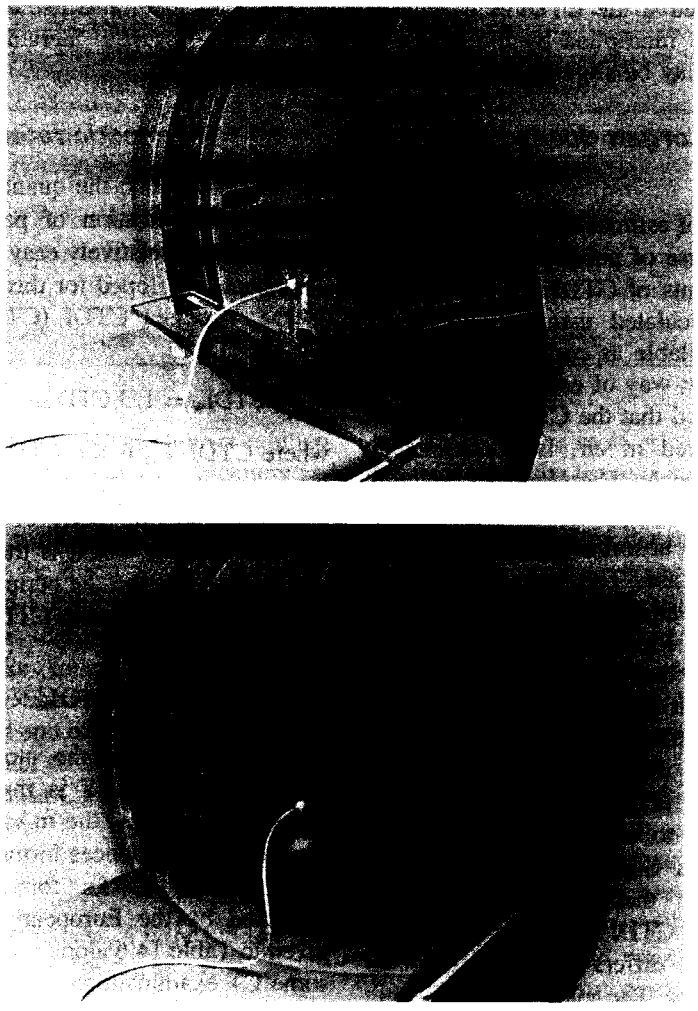

Figure 14.3 The set-up for measuring CTDI: (a) the 100 mm pencil ionisation chamber is positioned on-axis to measure CDTI free in air; (b) the chamber is inserted in a perspex phantom for a measurement in perspex. The phantom is 320 mm in diameter to simulate the body but the outer annulus can be removed to leave the central 160 mm diameter phantom to simulate the head. Four plugged cavities exist around the periphery of each phantom for additional measurements required to calculate $CTDI_w$.

customary to assign CT scanners an average energy of 70 keV (in a phantom) to aid in its determination. Apart from air, the most common medium used in CT dosimetry is perspex which has an approximate F value of 0.887. The ion chamber calibration should be undertaken at realistic beam qualities representative of CT practice.

CTDI can be measured free in air or in a suitable phantom, and either on the axis of rotation of the scanner or near the periphery of the phantom, depending on the purpose of the measurements (Figure 14.3). If performed in a phantom, it is equivalent to the average dose across the central scan width from several surrounding contiguous scans.

Phantoms suitable for dosimetry measurements are usually constructed from polymethylmethacrylate (acrylic or perspex), with a number of removable plugs for the insertion of TLDs or ionisation chambers. Standard diameters are 160 mm to simulate the head, and 320 mm for the body. The design has been recommended by the IEC and is described in more detail by Edyvean [25].

A CTDI value measured as described above depends on the usual factors, such as mAs, kV, and scanner geometry. It does not depend strongly on slice width, except that the smallest nominal slice width on a scanner may be determined by post-patient collimation, resulting in a higher CTDI compared with larger slice widths. Often it is useful to normalize the CTDI by dividing by the mAs. However, care needs to be taken if patient examination protocols employ overscan, since it is common for the scanner to give the nominal scan time for a 360° rotation, rather than the actual time. Thus, the

dose may be underestimated if the CTDI is calculated from the normalized CTDI multiplied by the indicated mAs, since the true mAs may be slightly greater.

14.8.2 Estimation of organ doses and effective dose

The most convenient way of estimating organ doses and effective dose is to make use of published data relating organ doses to measurements of CTDI per mAs in air. Such data have been calculated using Monte Carlo methods [20], and are available as computer data files, providing a very convenient way of estimating effective dose [26]. It should be noted that the CTDI required for the data, although measured in air, is quoted as an absorbed dose to ICRU muscle. Therefore, a correction factor of 1.07 will need to be applied if measurements have been made in terms of absorbed dose to air, or air kerma, as is usually the case. The normalized organ doses are scanner specific, and so a potential problem arises if doses are required for patients examined on a scanner introduced after the work of Jones and Shrimpton [20]. However, it may be possible to find a matched older scanner to estimate effective dose, based on a knowledge of the different scanner models, filtration, kV, and geometry [27].

It should be noted that to comply with regulatory requirements in the United States, CT manufacturers provide data on CTDI in their technical literature. However, the definition of CTDI used by the Federal Drug Administration (FDA) differs in some significant aspects from that used above. The main difference is in the integration limits, which are $\pm 7T$, where T is the slice thickness, rather than the ± 50 mm normally used for practical patient dose measurements. The two quantities will only agree for a slice thickness of 7 mm. $CTDI_{FDA}$ is determined in standard 16 cm and 32 cm diameter perspex phantoms, and is quoted as absorbed dose to perspex. In order to compare measurements of $CTDI_{100}$ made using a 100 mm pencil chamber with respect to air with values of $CTDI_{FDA}$ derived according to the FDA definition in perspex, correction factors given in Table 14.5 can be used. These factors allow measurements at acceptance to be compared with values quoted in the manufacturers' literature and can be used in dose evaluation.

14.8.3 Diagnostic reference levels (DRLs)

It is important that the quantities used for DRLs give a meaningful indication of patient exposure, yet at the same time are relatively easy to measure. Two quantities have been developed for this purpose, which are known as the weighted CTDI ($CTDI_w$) and the dose–length product (DLP).

$$CTDI_w = 1/3\ CTDI_{100,c} + 2/3\ CTDI_{100,p}\ \text{mGy}$$

where $CTDI_{100,c}$ is the CTDI measured with a 100 mm long pencil ionisation chamber at the centre of the standard phantom (body or head), and $CTDI_{100,p}$ is a similar quantity, which is the average of four measurements made around the periphery (i.e. 10 mm below the surface) of the phantom. $CTDI_w$ is expressed in terms of absorbed dose to air.

$$DLP = \sum_i {}_nCTDI_w \times T \times N \times C\ \text{mGy cm}$$

where ${}_nCTDI_w$ is the normalized weighted CTDI ($CTDI_w$ per mAs), T is the slice thickness, N is the number of slices, C the mAs per slice, and the sum i is over all scan sequences forming part of the examination.

Preliminary DRLs for adult patients have been proposed by the European Commission [28] and are given in Table 14.6 along with typical effective doses for some CT examinations.

14.8.4 Spiral CT

CTDI is not strictly defined for spiral or helical CT; however, for dose calculations it can be assumed to be the same as the value obtained for the corresponding standard axial scan, allowing for any overscan in the standard mode. When using the NRPB program to estimate effective dose, one can either use contiguous slices and divide the result by the pitch or choose a packing factor equal to the inverse of the pitch; the results are essentially the same. Here the pitch is defined

Table 14.5 Ratio of $CTDI_{FDA(perspex)}$ to $CTDI_{100(air)}$

Slice thickness (mm)	Head phantom			Body phantom		
	C	P	S	C	P	S
10	0.98	0.93	0.92	1.03	0.93	0.92
5	0.77	0.82	0.84	0.72	0.82	0.82
3	0.62	0.74	0.76	0.53	0.74	0.75
2	0.49	0.67	0.71	0.38	0.67	0.71
1.5	0.45	0.63	0.67	0.34	0.61	0.67
1	0.32	–	–	0.26	–	–

C, P, and S represent measurement positions at the centre, periphery (1 cm deep), and surface of the CTDI phantoms.

Table 14.6 Typical patient doses and provisional diagnostic reference levels for computed tomography

Examination	Effective dose (mSv)	Diagnostic reference level $CTDI_w$ (mGy)	DLP (mGy cm)
Head	2	60	1050
Chest	8	30	650
Abdomen	10	35	800
Pelvis	10	35	600
Liver and spleen	10	35	900
HRCT lung	3.5	35	280
Vertebral trauma	7.5	70	460
Face and sinuses	0.6	35	360

as the distance travelled by the couch per tube revolution, divided by the product of the nominal slice thickness and number of sections produced in a single tube rotation. It should be noted that some manufacturers use a different definition of pitch, namely the distance travelled by the couch per rotation, divided by the single slice detector aperture. According to this definition the pitch for a scanner collecting data for four simultaneous slices would be four times greater. Usually, additional scanning is performed at the start and end of a run for interpolation purposes, although for normal scan lengths the additional dose is insignificant. For spiral CT the equation for DLP needs to be modified slightly:

$$\mathrm{DLP} = \sum_i {}_n\mathrm{CTDI_w} \times T \times A \times t \text{ mGy cm}$$

where T is the nominal slice thickness, A is the tube current, and t is the total acquisition time for the sequence.

14.8.5 Scan projection radiography (SPR)

SPR may be used to aid alignment and select the region to be scanned in cross-sectional imaging. In such cases the contribution to the total dose from the examination is very small and is usually ignored. SPR may also be used as a very low dose technique where the diagnostic features do not depend on high image quality, e.g. pelvimetry. In such applications the usual techniques for measuring doses in conventional radiography can be used. The dose will depend on factors such as the mA, couch speed, and slice width.

14.9 Specialist radiographic techniques

14.9.1 Mammography

In mammography the only part of the body which receives a significant dose is the breast itself. It is therefore usually unnecessary and irrelevant to estimate effective dose. The ICRP has recommended that the mean absorbed dose to the glandular tissue (including the ductal and acinar epithelium) is the most relevant dose quantity. However, the term glandular tissue is imprecise and Bryant *et al.* [29] have indicated that the volume of tissue at risk is much lower than implied by the standard breast model.

Particularly since screening for breast cancer has become widespread, standard protocols for dose measurements have been developed [30]. Although suitably calibrated TLDs can be used with standard perspex or breast tissue equivalent phantoms, they will be visible on mammograms if used on patients, and there may be some uncertainty as to whether backscatter is fully detected. Instead, the method of choice is by calculation from recorded exposure factors and output measurements. The relationship between mean glandular dose (MGD) and incident air kerma has been derived from Monte Carlo calculations [31] and is a function of beam quality, i.e. half-value layer and anode–filter combination, breast thickness, and breast composition (Box 14.6). Incident air kerma is easily derived from output measurements, taking care to undertake these with the breast compression plate in position. Breast composition can be estimated by inspection of the mammograms, although, relative to the standard 50% glandular–50% adipose composition, the correction does not amount to more than about 20%. Factors to convert incident air kerma to MGD can be found in the aforementioned protocols.

Measurements on groups of women in the UK National Breast Screening Programme have indicated a median MGD for the mediolateral oblique view of 1.7 mGy, with an interquartile range of 1.2–2.4 mGy [32]. Corresponding figures for the craniocaudal view were 1.4 mGy for the median, and 1.1–2.0 mGy for the interquartile range. These figures should not be confused with the MGD for the standard breast (40 mm perspex), which is used for quality control purposes and tends to be somewhat lower than doses measured on real women.

14.9.2 Dental radiography

Although the effective dose from a dental exposure is small, the frequency of dental radiography is very high, resulting in an annual collective dose of about 200

manSv in the UK. Unfortunately, projections and exposure parameters relevant to dental radiography are not available in the commonly used software packages for estimating organ and effective doses.

A number of workers have used sectioned head phantoms with TLD inserts to estimate the absorbed dose to the different organs in the head, and hence the effective dose. Doses are usually small and multiple exposures are generally needed. The estimation of effective dose needs careful consideration in view of the fact that much of the dose is to 'remainder' organs.

Dose estimation in panoral radiography raises two further problems, namely the narrow slit shape of the X-ray beam makes it difficult to make measurements of output or kV, and also the dose distribution inside the head is very non-uniform, making it difficult to estimate dose to organs. Figure 14.4 shows a typical dose distribution as measured by a film inserted between slices of a Rando head phantom. Together with a TLD, this can give a more complete picture of the dose. It is interesting to note the hot spot at the salivary glands, which is neither an ICRP organ with a specified weighting factor nor one of the named remainder organs. Frederiksen *et al.* [33] have considered the implications for effective dose including the salivary glands in the calculation and concluded that they contribute 61% of the total effective dose.

Box 14.6 Calculation of mean glandular tissue dose in mammography

The mean glandular tissue dose (MGD) can be calculated from the incident air kerma (K) at the breast surface. A 40-mm-thick perspex phantom with the same cross-sectional area as the standard breast is used in the UK [30] and European protocols to check and compare the dose performance of mammography units. The standard phantom equates to a 45-mm-thick breast and it is assumed that the composition is 50% glandular tissue and 50% adipose tissue for calculation of MGD using the equation:

$$\text{MGD} = K\ p\ g\ s$$

where the factor p converts air kerma for the perspex phantom to that for the standard breast and g converts air kerma for the standard breast to the mean glandular tissue dose for X-ray spectra obtained from a molybdenum target used with a molybdenum filter characterized by the half-value layer (HVL) in aluminium (Table B14.1) [30]. The factor s corrects for X-ray spectral differences arising from the use of alternative target/filter combinations (Table B14.2) [31].

Table B14.1 Conversion factors p and g for calculating the mean glandular tissue dose to the standard 40-mm-thick perspex phantom for different beam HVLs

HVL (mm Al)	0.30	0.35	0.40	0.45	0.50
p	1.10	1.10	1.09	1.09	1.09
g (mGy/mGy)	0.183	0.208	0.232	0.258	0.285

Table B14.2 s-factors for X-ray spectra used clinically

Anode/filter materials	s-factor
Mo/Mo	1.00
Mo/Rh	1.017
Rh/Rh	1.061
Rh/Al	1.044
W/Rh	1.042

Determination of MGDs for individual patients requires account to be taken of different breast thicknesses and the percentage of glandular tissue. The assumption of 50% glandularity is approximately correct for breast thicknesses of 40–60 mm, but not for thinner or thicker ones. For this an equation of the form:

$$\text{MGD} = \text{K g c s}$$

can be used, which includes an additional factor c related to the glandularity of the tissue. Values for the g-factor for a range of breast thicknesses have been derived from Monte Carlo simulation and are given in Table B14.3.

For intra-oral radiography, the DRL is most conveniently given in terms of the patient entrance dose per film, without backscatter, or in other words the dose in air at the end of the spacer cone. For panoramic radiography a different reference dose quantity is required because of the difficulty in defining a simple method for measuring patient dose resulting from the rotation of the X-ray tube. Dose detectors which are sufficiently narrow to lie entirely within the X-ray beam are now available for measuring the output from these units. The method proposed for dose assessment is based on the dose–width product, that is the product of the total dose per exposure cycle at the slot at the cassette carriage faceplate and the beam width at that position. The NRPB has recommended DRLs of 4 mGy for an adult mandibular molar intra-oral radiograph, and 65 mGy mm for a standard adult panoramic radiograph [34] (Table 14.7). However, in the future DAP is likely to be the dose quantity of choice in panoramic radiography.

14.9.3 Paediatric radiography

Paediatric doses can vary tremendously due to the great variation in the size of patients, from neonates to adult-sized teenagers. Because the risk of harmful radiation effects is higher than in adults, the need to minimize doses is of paramount importance. Also, the smaller body size means that precise collimation can be more difficult,

***Box 14.6** (continued)*

There is a close relationship between glandularity and breast thickness for women within particular age groups, which enables standard values to be assumed [31]. The percentage glandularity for women with different breast thicknesses in age groups examined frequently are given in Table B14.4, together with values for the c-factor for different beam HVLs and these values can be substituted directly into the above equation. Data for a wider range of HVLs and breast thicknesses can be found in [31]. If more than one film is required, because of the size of the breast, the MGD will be approximately proportional to the number of films, because the region of overlap is usually quite large.

Table B14.3 g-factors (mGy/mGy) as a function of compressed breast thickness for different X-ray beam HVLs

Breast thickness	HVL (mm Al)			
(mm)	0.30	0.35	0.40	0.45
20	0.390	0.433	0.473	0.509
30	0.274	0.309	0.342	0.374
40	0.207	0.235	0.261	0.289
50	0.164	0.187	0.209	0.232
60	0.135	0.154	0.172	0.192
70	0.114	0.130	0.145	0.163
80	0.098	0.112	0.126	0.140

Table B14.4 Average breast composition and values for c-factors for average breasts for women in two age groups, as a function of compressed breast thickness

	Women aged 40-49 years					Women aged 50-64 years				
Breast thickness	Gland ularity	c-factors for various unit HVLs (mm Al)				Gland ularity	c-factors for various unit HVLs (mm Al)			
(mm)	(%)	0.30	0.35	0.40	0.45	(%)	0.30	0.35	0.40	0.45
20	100	0.885	0.891	0.900	0.905	100	0.885	0.891	0.900	0.905
30	82	0.894	0.898	0.903	0.906	72	0.925	0.929	0.931	0.933
40	65	0.940	0.943	0.945	0.947	50	1.000	1.000	1.000	1.000
50	49	1.005	1.005	1.005	1.004	33	1.086	1.082	1.081	1.078
60	35	1.080	1.078	1.074	1.074	21	1.164	1.160	1.151	1.150
70	24	1.152	1.147	1.141	1.138	12	1.232	1.225	1.214	1.208
80	14	1.220	1.213	1.206	1.205	7	1.275	1.265	1.257	1.254

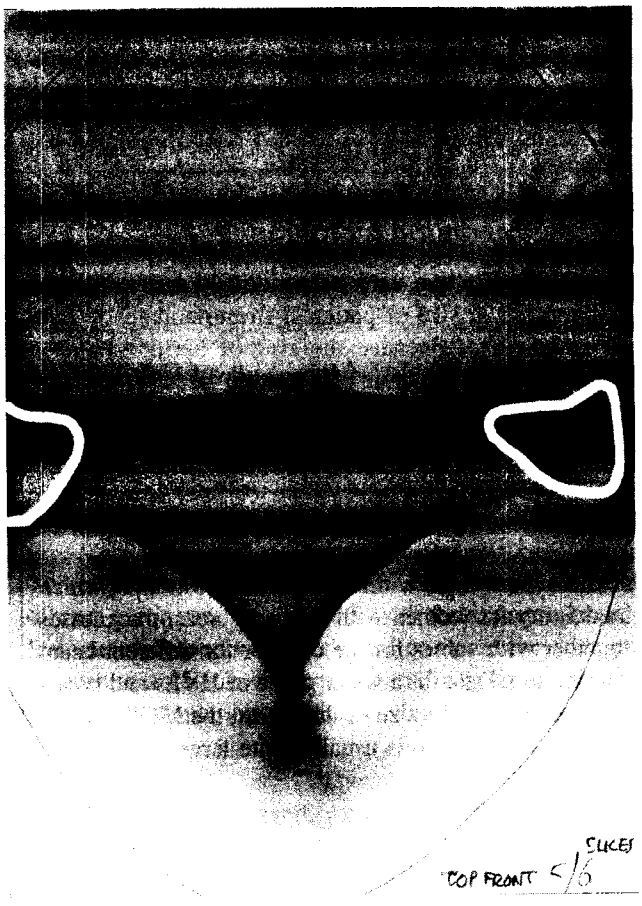

Figure 14.4 The dose distribution from a Planmeca Proline panoramic dental unit, obtained by exposing a non-screen film inserted between sections 5 and 6 of a Rando head phantom. The positions of the parotid glands are outlined in white. The effective rotating centre of the X-ray beam starts just outside the head, alongside the parotid gland, and follows a curved path coinciding with the lower edge of the most exposed area of the film.

and more organs are likely to be within, or close to, the direct beam.

In general, the same techniques as described for adults can be used for estimating radiation dose, the main difference being that the doses are usually much less. For example, ESDs are typically in the range 0.1–0.5 mGy, and down to 0.02 mGy for chest examinations. Similarly, DAP readings may be only a few mGy cm^2. As indicated in §14.6.2, Monte Carlo generated data are available for estimating organ and effective doses for a range of paediatric examinations, although CT is a notable exception.

Typical figures for ESD and DAP can be ascertained by surveying the literature, although fewer large-scale paediatric studies have been performed compared with those undertaken on adults. DRLs for simple radiographic examinations have been proposed by the European Commission [35] and are reproduced in Table 14.8 along with typical doses. Insufficient data are currently available to enable corresponding reference levels to be developed for the more complex procedures involving fluoroscopy. Clearly, further work is also required to develop a framework for dealing with patients of different sizes. One possibility might be to derive a relationship between patient dose and size, and then use this to normalize doses to a fixed patient size. For instance, Martin *et al.* [36] have proposed the use of an 'equivalent diameter', calculated from patient weight and height, which could allow doses for children of different ages to be compared with the appropriate reference levels.

14.10 Bone mineral densitometry

Bone density measurements can be made using a variety of techniques, such as radiographic absorptiometry (RA), single X-ray absorptiometry (SXA), dual X-ray absorptiometry (DXA), and quantitative computed tomography

Table 14.7 Typical patient doses and provisional diagnostic reference levels for dental radiography

Examination	Effective dose (μSv)	Entrance surface dose (mGy)	Diagnostic reference level[a] (mGy)
Bitewing, rectangular collimation, E speed film,[b] 70 kV, 200 mm FSD	1	1.8[c]	4
Bitewing, round collimation, E speed film,[b] 70 kV, 200 mm FSD	2	1.8[c]	4
Bitewing, round collimation, E speed film,[b] 50–60 kV, 100 mm FSD	4	4.1	4
Panoramic radiography	7		65 mGy mm[d]

[a]Dose in air at the end of the cone.
[b]The use of D speed film would double the dose from the intra-oral films.
[c]The figure of 1.8 mGy is an average for a survey which included both types of collimation.
[d]Product of total dose and slit width.

Table 14.8 Typical patient doses and provisional diagnostic reference levels for paediatric procedures

Examination	Age (years)	ESD (μGy)	Effective dose (μSv)	Diagnostic reference level[a] (μGy)
Abdomen AP/PA	1	329	69	400
Abdomen AP/PA	5	479	70	500
Abdomen AP/PA	10	756	103	800
Abdomen AP/PA	15	1287	122	1200
Chest AP	0	59	15	50
Chest AP/PA	1	44	5.5	50
Chest AP/PA	5	55	6.6	70
Chest AP/PA	10	88	6.3	120
Chest LAT	5			200
Pelvis AP (no grid)	0	49	5.8	200
Pelvis AP	1	388	45	500
Pelvis AP	5	445	63	600
Pelvis AP	10	713	50	700
Pelvis AP	15	1577	142	2000
Skull AP/PA	1	736	14	800
Skull AP/PA	5	910	11	1100
Skull LAT	1	476	8.5	500
Skull LAT	5	573	8	800

[a]Entrance surface dose.
DRLs based on European Commission [34] adapted to the UK.

(QCT). The most common techniques are probably DXA and QCT, although the other methods are gaining in popularity due to recent technical developments. With the exception of QCT, specialized equipment is needed. In the case of DXA, a pencil or fan beam of X-rays scans the area of interest, commonly the lumbar spine, proximal femur, or whole body. The energy of the beam is rapidly switched, either by changing the filtration or by changing the kV, resulting in a relatively hard beam compared with general radiography. This, together with the scanning geometry and size of the X-ray beam, will need to be considered when making measurements of patient dose.

Most dose estimations reported in the literature have been based on ESD measurements or scans of anthropomorphic phantoms loaded with TLDs. In order to determine effective dose, ESD measurements can be combined with depth dose data and anatomical information to derive organ doses, and hence effective dose. The doses are, however, very low and many scans will be needed to give measurable readings with TLDs in a phantom. Standard techniques, already described, can be used for estimating the dose from QCT.

As can be seen from Table 14.9, patient doses can vary considerably, depending on equipment design, scanning mode, and area of the body, but are generally very much lower than those arising from general radiography. Similarly, the doses from QCT are much lower than those from imaging CT. For further details the reader is referred to a review of techniques and doses,

Table 14.9 Typical patient doses in bone densitometry

	Entrance surface dose (μGy)	Effective dose (μSv)
DXA pencil beam		
spine	10–60	0.2–0.5
femur	10–60	0.02–0.1
whole body	10–20	4
DXA fan beam		
spine	60–900	0.4–75
femur	140–900	0.3–18
whole body	10–900	2.7–41
QCT spine	3000	60–500

The large differences are mainly due to differences in equipment design.
The above effective doses exclude the contribution from the ovaries, as may apply in postmenopausal women. In many instances it is not clear whether the ovaries will be in the X-ray beam or not.

including relevant references, published by Njeh *et al.* [37]. DRLs have not yet been developed for bone mineral densitometry.

14.11 Pregnancy and the estimation of fetal dose

Occasions arise where pregnant patients undergo X-ray examinations, either intentionally because the examination is required urgently for the management of the patient or inadvertently because the patient was unaware that she was pregnant at the time of the examination. Advice is available to clinical radiology departments on exposure to ionising radiation during pregnancy for dealing with such situations and this is summarized in Box 11.3.

Two common reasons for estimates of fetal dose to be required are as follows. First, individual X-ray departments need to know which of their procedures and techniques would give a dose to the fetus of tens of mGy (Box 11.3) and therefore require an examination to be scheduled in the first 10 days of the menstrual cycle. Second, whenever a pregnant patient is X-rayed it is usually necessary to estimate the fetal dose 'for the record', even though it is extremely unlikely that the dose would pose a significant risk or require any change in the management of the patient. The only routine examinations for which rescheduling is likely to be required are CT of the pelvis and abdomen and possibly barium enemas.

In the circumstances described above, in early pregnancy, it is relatively straightforward to estimate the dose to the fetus, since it can be assumed that the dose to the uterus will be a good estimate of the fetal dose, and the techniques already described for organ doses can be used. In later pregnancy the mean depth dose of the fetus will be greater and the ratio between effective dose and ESD or DAP will decrease accordingly. Adjustments may be made to the fetal dose based on depth dose data.

14.12 References

1 Hart, D., Jones, D. G., and Wall, B. F. (1994). *Estimation of effective dose in diagnostic radiology from entrance surface dose and dose–area product measurements.* NRPB-R262. NRPB, Chilton.

2 Hart, D., Jones, D. G., and Wall, B. F. (1996). *Coefficients for estimating effective doses from paediatric X-ray examinations.* NRPB-R279. NRPB, Chilton (and CHILDOSE program).

3 Harrison, R. M. (1982). Backscatter factors for diagnostic radiology (1–4 mm Al HVL). *Phys. Med. Biol.*, **27**, 1465–73.

4 Harrison, R. M. (1981). Central-axis depth–dose data for diagnostic radiology. *Phys. Med. Biol.*, **26**, 657–70.

5 Harrison, R. M. (1983). Tissue–air and scatter–air ratios for diagnostic radiology (1–4 mm Al HVL). *Phys. Med. Biol.*, **28**, 1–18.

6 ICRP (1996). Radiological protection and safety in medicine. ICRP Publication 73. *Ann. ICRP*, **26** (2).

7 European Commission (1997). Council Directive 97/43/Euratom of 30 June 1997 on health protection of individuals against the dangers of ionising radiation in relation to medical exposure, and repealing Directive 84/466/Euratom. *Off. J. Eur. Communities*, No. L180/22. EC, Luxembourg.

8 Health and Safety Executive (1999). *The Ionising Radiations Regulations 1999.* SI 1999 No. 3232. HMSO, London.

9 Department of Health (2000). *The Ionising Radiation (Medical Exposure) Regulations 2000.* SI 2000 No. 1059. HMSO, London.

10 Health and Safety Executive (1998). *Fitness of equipment used for medical exposure to ionising radiation.* Guidance Note PM77 (2nd edn) (under revision). HMSO, London.

11 International Commission on Radiation Units and Measurements (1989). *Tissue substitutes in radiation dosimetry and measurement.* Report 44. ICRU, Bethesda, MD, USA.

12 International Commission on Radiation Units and Measurements (1992). *Phantoms and computational models in therapy, diagnosis and protection.* Report 48. ICRU, Bethesda, MD, USA.

13 International Electrotechnical Commission (1994). *Medical diagnostic X-ray equipment–radiation conditions for use in determination of characteristics.* IEC 61267 (1994-10). IEC, Geneva.

14 Wagner, L. K., Fontenia, D. P., Kimme-Smith, C., Rothenberg, L. N., Shepherd, J., and Boone, J. M. (1992). Recommendations on performance characteristics of diagnostic exposure meters: report of AAPM Diagnostic X-ray Imaging Task Group No. 6. *Med. Phys.*, **19**, 231–41.

15 Burke, K. and Sutton, D. (1997). Optimisation and deconvolution of lithium fluoride TLD-100 in diagnostic radiology. *Br. J. Radiol.*, **70**, 261–71.

16 Andreo, P. (1991). Monte Carlo techniques in medical radiation physics. *Phys. Med. Biol.*, **36**, 861–920.

17 Morin, R. (1988). *Monte Carlo simulation in the radiological sciences.* CRC Press, Florida.

18 Jones, D. G. and Wall, B. F. (1985). *Organ doses from medical X-ray examinations calculated using Monte Carlo techniques.* NRPB-R186. NRPB, Chilton.

19 Hart, D., Jones, D. G., and Wall, B. F. (1994). *Normalised organ doses for medical X-ray examinations calculated using Monte Carlo techniques.* NRPB-SR262. NRPB, Chilton. The XDOSE program, available from J. C. Le Heron, National Radiation laboratory, Ministry of Health, Christchurch, New Zealand, utilizes the NRPB data to calculate organ doses and effective doses.

20 Jones, D. G. and Shrimpton, P. C. (1991). *Survey of CT practice in the UK Part 3: normalised organ doses calculated using Monte Carlo techniques.* NRPB-R250. NRPB, Chilton.

21 Spiers, F. W. (1988). Bone and bone marrow dosimetry. In: *Patient dosimetry in diagnostic radiology*, Chapter 5. IPSM Report No. 53. IPSM, York.

22 IPSM/NRPB/CoR (1992). *National protocol for patient dose measurements in diagnostic radiology.* NRPB, Chilton.

23 Rosenstein, M., Suleiman, O. H., Burkhart, R. L., Stern, S. H., and Williams, G. (1992). *Handbook of selected tissue doses for the upper gastrointestinal fluoroscopic examination.* HHS

Publication FDA 92–8282. US Department of Health Education and Welfare, Rockville, MD, USA.

24 Stern, S. H., Rosenstein, M., Renaud, L., and Zankl, M. (1995). *Handbook of selected tissue doses for fluoroscopic and cineangiographic examination of the coronary arteries.* HHS Publication FDA 95–8289. US Department of Health Education and Welfare, Rockville, MD, USA.

25 Edyvean, S. (1998). *Type testing of CT scanners: methods and methodology for assessing imaging performance and dosimetry.* MDA Evaluation Report MDA/98/25. Department of Health, London.

26 Jones, D. G. and Shrimpton, P. C. (1991). *Normalised organ doses for X-ray computed tomography calculated using Monte Carlo techniques.* NRPB-SR250. NRPB, Chilton. The CTDOSE program, available from J. C. Le Heron, National Radiation laboratory, Ministry of Health, Christchurch, New Zealand, utilizes the NRPB data to calculate organ doses and effective doses.

27 ImPACT (1999). *Imaging performance assessment of CT scanners.* Medical Physics Department, St George's Hospital, London. http://www.impactscan.org/scannermatching.htm.

28 European Commission (1999). *European guidelines on quality criteria for computed tomography.* EUR 16262 EN. EC, Luxembourg.

29 Bryant, R. J., Underwood, A. C., Robinson, A., Stephenson, T. J., and Underwood, J. C. E. (1998). Determination of breast tissue composition for improved accuracy in estimating radiation doses and risks in mammographic screening. *The Breast*, **7**, 95–8.

30 IPSM (1994). *The commissioning and routine testing of mammographic X-ray systems.* Report No. 59 (2nd edn) (under revision). IPSM, York.

31 Dance, D. R., Skinner, C. L., Young, K. C., Beckett, J. R., and Kotre, C. J. (2000). Additional factors for the estimation of mean glandular breast dose using the UK mammography dosimetry protocol. *Phys. Med. Biol.*, **45**, 3225–40.

32 Burch, A. and Goodman, D. A. (1998). A pilot survey of radiation doses received in the United Kingdom Breast Screening Programme. *Br. J. Radiol.*, **71**, 517–27.

33 Frederiksen, N. L., Benson, B. W., and Sokolowski, T. W. (1994). Effective dose and risk assessment from film tomography used for dental implant diagnostics. *Dentomaxillofac. Radiol.*, **23**, 123–7.

34 Napier, I. D. (1999). Reference doses for dental radiography. *Br. Dent. J.*, **186**, 392–6.

35 European Commission (1996). *European guidelines on quality criteria for diagnostic radiographic images in paediatrics.* EUR 16261 EN. EC, Luxembourg.

36 Martin, C. J., Farquhar, B., Stockdale, E., and Macdonald, S. (1994). A study of the relationship between patient dose and size in paediatric radiology. *Br. J. Radiol.*, **67**, 864–71.

37 Njeh, C. F., Fuerst, T., Hans, D., Blake, G. M., and Genant, H. K. (1999). Radiation exposure in bone mineral density assessment. *Appl. Radiat. Isot.*, **50**, 215–36.